Journal of South American Earth Sciences 130 (2023) 104570

Contents lists available at ScienceDirect

Journal of South American Earth Sciences

journal homepage: www.elsevier.com/locate/jsames

The Neoproterozoic Agudos Grandes granitic batholith, SE Brazil: Inferences on source areas from elemental and Sr-Nd-Pb isotope geochemistry

Valdecir de Assis Janasi [a,*], Lucelene Martins [a], Adriana Alves [a], Antonio Simonetti [b], Renato Henrique-Pinto [a]

[a] Instituto de Geociências, Universidade de São Paulo, 05508-080, São Paulo, SP, Brazil
[b] Department of Civil and Environmental Engineering and Earth Sciences, University of Notre Dame, Notre Dame, IN 46556, USA

ARTICLE INFO

Keywords:
Granite batholith
Sr-Nd-Pb isotope geochemistry
High-K calc-alkaline
U–Pb geochronology

ABSTRACT

I-type, K-rich calc-alkaline hornblende-biotite granitoids (HKCA) suites are typical of both pre- and post-collisional tectonic settings, and their petrogenesis is challenging, since they are dominated by rocks with intermediate composition (e.g., 60–68 wt% SiO_2; 10–20 vol % mafic mineral) that are neither typical products of crust nor of mantle partial melting. These granitoids are particularly abundant as the main components of Ediacaran batholiths intruding the Neoproterozoic Ribeira Fold Belt in SE Brazil, e.g. constituting ~70% of the exposition of the Agudos Grandes Batholith, where they were emplaced at 620-610 Ma, as indicated by U–Pb zircon dating from our previous work and new data presented here. Two types of coeval granitoids comprise an expanded suite of mafic to felsic titanite and allanite-rich biotite granitoids (Itapevi-type) and a single occurrence of biotite-muscovite leucogranite (Turvo-type). Elemental and isotope whole-rock data indicate that different sources were involved in the genesis of their parent magmas, with crust with old residence predominating for the HKCA and Itapevi types, as indicated by very negative (−16 to −20) εNd(t) and low initial $^{206}Pb/^{204}Pb$ (16.4–16.7), and younger metasedimentary rocks as the source of the Turvo leucogranite (εNd(t) (~-14); initial $^{87}Sr/^{86}Sr = 0.717$). This "syn-orogenic" magmatism was immediately followed, as demonstrated by field and geochronological data, by ~605-600 Ma circumscribed plutons dominated by more fractionated (±muscovite)-biotite granites that derive from melts generated in the middle crust from sources that are slightly younger than those of the HKCA granitoids, as indicated by slightly less negative (εNd(t) (similar to those of the Turvo leucogranite) and higher $^{206}Pb/^{204}Pb$ (17.1–17.3). After a ~15 Myr lull, A-type plutons were emplaced in a post-orogenic setting, probably from mantle and crust sources. The syn-to late-orogenic (620-600 Ma) magmatism of the Agudos Grandes was produced by a thermal anomaly, probably associated with a continental arc. A combination of elemental and isotope geochemistry and inherited zircon data suggests that crustal melting was probably induced by ascension of mantle-derived basic magmas, and initiated in hot zones at the lower portions of a previously thickened crust, formed by old Paleoproterozoic to Archean material (the basement of the Apiaí-São Roque Domain of the Ribeira Belt?), and progressed to the middle portions of the crust, where it provoked partial melting of a different crustal domain with younger age and crustal residence (Embu Complex orthogneisses and metasediments).

1. Introduction

Metaluminous granitoids with calc-alkaline affinity ("I-type granites") are conspicuous magmatic products of convergent tectonics, and their significance is still controversial from both the tectonic and petrologic perspectives (Castro, 2014; Clemens et al., 2011; Collins et al., 2016; Jacob et al., 2021). Although they are the archetype plutonic components of continental arc magmatism, fairly similar granites also occur in the post-collisional setting, and much effort has been spent to find reliable parameters allowing distinguish between

* Corresponding author.
E-mail addresses: vajanasi@usp.br (V.A. Janasi), lucemart@usp.br (L. Martins), adrianaalves@usp.br (A. Alves), simonetti.3@nd.edu (A. Simonetti), renatohp@usp.br (R. Henrique-Pinto).

https://doi.org/10.1016/j.jsames.2023.104570
Received 11 July 2023; Received in revised form 28 August 2023; Accepted 28 August 2023
Available online 29 August 2023

calc-alkaline granites (usually K-rich) generated in these two contrasting (but often overlapping in time and space) tectonic environments, and identify the sources involved. Uncertainties arising from these similarities may be already difficult to disentangle in young orogens (see for instance Hildebrand and Whalen, 2017), and predictably get stronger in Precambrian mobile belts where relations with present tectonic configuration are less evident or remains poorly constrained.

The complex orogenic systems that make up the Neoproterozoic orogens in SE Brazil, related to amalgamation of Western Gondwana, comprise a puzzle of diverse terrains, many of them intruded by voluminous granite batholiths dominated by I-type suites that are relatively expanded compositionally, and are typically potassium-rich ("high-K calc-alkaline", hereafter abbreviated HKCA). A direct relationship with ocean-plate consumption (arc-type magmatism *sensu strictu*) is admitted by many authors, at least for the oldest, often deformed manifestations, but in many cases no unequivocal markers of oceanic closure and ensuing collision are identified, and a same HKCA granite suite may happen to be considered as pre-collisional or post-collisional by different authors. The superposition of collisional events, and the diachronic character of a single collisional event further complicate the picture.

This paper is a contribution to the petrogenesis of one such expressive manifestation of HKCA granite magmatism in the Ribeira Fold Belt in the Mantiqueira Province (Heilbron et al., 2004). The Agudos Grandes Batholith has been subject of some previous publications of our group, which emphasized the chronostratigraphy of magmatism, and focused on the late- and post-orogenic manifestations, that were emplaced in the period of 605-565 Ma, during which the character of magmatism changed from HKCA (to a large extent showing evidence of strong contamination by crustal sources; see Leite et al., 2006, 2007a,b) to A-type (with metaluminous character). The typical metaluminous I-type HKCA granites that make up most of the batholith occur as elongated bodies, described as "syn-orogenic", and were shown to have ages just slightly older (≥610 Ma) than the first circumscribed late-orogenic plutons, but thus far were not studied in detail. We try to fill this gap by presenting a study of these rocks and other granite types shown to be coeval with them, using whole-rock elemental and Sr–Nd isotope geochemistry. An integrated model for the genesis and evolution of the Agudos Grandes magmatism is presented using the whole geochemical dataset, supplemented by K-feldspar Pb isotope data for a set of granite samples comprising the full temporal and compositional range recognized in the Agudos Grandes Batholith.

2. Geological context

Large volumes of granitic magmatism, dominated by high-K calc-alkaline granitoids forming elongated batholiths, is a main feature of the fold belts generated during the Neoproterozoic orogenic processes in SE Brazil. One of the largest granite occurrences is the Agudos Grandes Batholith, which extends for over 200 km roughly in a N60E direction west of the city of São Paulo, intruding low-to medium-grade metavolcanosedimentary sequences in the Embu Domain (Fig. 1).

Dextral strike-slip shear zones resulting from oblique tectonics (Campanha and Brito Neves, 2004), resulted in a mosaic of block-faulted domains which juxtapose contrasted rock associations. The Embu Domain is defined as a block within the Ribeira Fold Belt, located between the low-to medium-grade, mostly passive-margin metavolcanosedimentary sequences of Mesoproterozoic to Neoproterozoic age of the São Roque Domain and the dominantly high-grade, mostly Ediacaran-age migmatites and orthogneisses of the Coastal Domain (e.g., Heilbron et al., 2004). Three main sequences are recognized in the Embu Domain: locally exposed windows of Paleoproterozoic migmatites (e.g., the Rio Capivari Complex; Maurer et al., 2015); medium- to high-grade metamorphic sequences with depositional age constrained by detrital zircon and metamorphism between 0.95 and 0.80 Ga (the Embu Complex of Hasui and Sadowski, 1976) and a low-grade metavolcanosedimentary sequence with a depositional age ~1.4–1.3 Ga (the Pilar do Sul Complex of Hasui and Sadowski, 1976, correlated with the Votuverava Group by Campanha et al., 2019), exposed in the W-NW portion of the Domain (Fig. 1).

Juxtaposition of the two contrasted meta-supracrustal sequences (Embu and Votuverava), probably by collision tectonics, occurred at ~0.8 Ga, as constrained by the presence of intrusive orthogneisses (Meira et al., 2015; Passarelli et al., 2019) and a widespread metamorphic event at this age in both units (Cabrita et al., 2021). Subsequent (680-580 Ma) magmatism is related to younger plate margin (subduction-collision) events that record the amalgamation of western Gondwana. South and east of the Agudos Grandes batholith, the granite magmatism of the Embu Domain is dominated by ~600-590 Ma porphyritic biotite granites and equigranular muscovite-biotite granites that intrude the Embu Complex. Elemental and Sr-Nd-Pb isotope geochemistry along with inherited zircon ages, indicate that these granites derive from crustal sources with composition from the Embu Complex and its basement (Alves et al., 2016). The Agudos Grandes

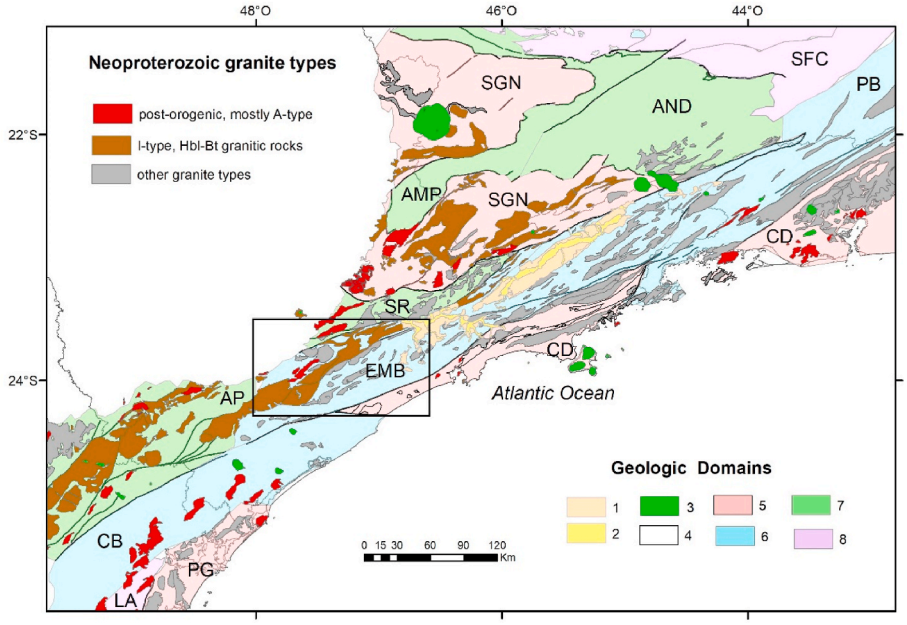

Fig. 1. Geological sketch of SE Brazil with main Neoproterozoic granitic occurences. Geologic domains: 1- Quaternary sediments, 2- Tertiary sediments; 3- Cretaceous alkaline rocks; 4- Phanerozoic sedimentary rocks; 5 to 8: Proterozoic to Archean Domains: 5: High-grade metamorphic domains with predominant orthogneisses of Neoproterozoic age: SGN= Socorro-Guaxupé Nappe; CD= Coastal Domain; PN= Paranaguá Domain; 6: CB= Curitiba; EMB = Embu; PB= Paraíba domains; 7: AP = Apiaí; SR= São Roque; AND = Andrelândia; AMP= Amparo domains; 8, SFC= São Francisco Craton; LA = Luiz Alves Craton. Area of Fig. 2 shown by the rectangle.

magmatism contrasts sharply with this magmatism, by the predominance of metaluminous hornblende-biotite granitoids and slightly older ages of the main volumes of granite (620-600 Ma; Janasi et al., 2001; Leite et al., 2007a; this work).

3. Geology and petrography

Fig. 2 is a simplified map of the eastern half of the Agudos Grandes Batholith, which is made up of a series of individual plutons with varied composition.

3.1. Syn-orogenic granitic magmatism

The syn-orogenic magmatism corresponds to the most expressive portion of the Agudos Grandes, and is formed by three distinctive granite associations (see Table 1 for the hierarchy adopted). Two occurrences (Ibiúna and Turvo) were previously dated at ~610 Ma (Janasi et al., 2001).

The first granite association consists of the predominant rock type in the Agudos Grandes batholith, a porphyritic hornblende-biotite quartz monzonite to monzogranite of high-K calc-alkaline (HKCA) affinity, which makes up several elongated bodies, and are here grouped in three types.

The most expressive **Ibiúna-type** makes up, from west to east, the Jurupará, Ibiúna and Cotia plutons. It is a relatively mafic granitoid (M = 10–15) with large K-feldspar megacrysts (usually 3–4 cm) set in a medium-to coarse-grained matrix where white plagioclase is the dominant feldspar. Mafic microgranular enclaves are present in a few exposures, but are not abundant. The rock is isotropic to slightly foliated in the Jurupará massif and in the central portions of the Ibiúna massif. A foliated, more felsic border facies, with smaller K-feldspar megacrysts (ca. 2 cm), is present in parts of the Ibiúna massif. Towards east (Cotia pluton), these rocks are increasingly more deformed and tend to occur as elongated tabular bodies. The augen-gneisses cropping out west of the city of São Paulo correspond to the Butantã-type of Coutinho (1972) and are interpreted as extremely deformed varieties of the Ibiúna-type granites.

A slightly more felsic variety of HKCA hornblende-bearing granite makes up the **Tapiraí-type**, and occurs along an extensive (up to 80 km long) strip oriented N60E north of the Jurupará pluton. This granite is petrographically similar to the border facies of the Ibiúna massif (a porphyritic hornblende-biotite monzogranite with 1–2 cm pink K-feldspar megacrysts), being distinguished by its lower M (ca. 8–10).

A third variety of porphyritic hornblende-biotite granite forms a pluton of ellipsoidal shape north of the Tapiraí-type granite strip in the westernmost part of the map. The **Rio Taquaral** pluton extends for at least 40 km with a maximum length of 12 km. In aerogammaspectrometic maps, it is marked by low Th and U signals (Ferreira et al., 1991).

A second granite association is also mostly metaluminous, but differs from the HKCA association by its strong foliation, inequi to equigranular texture, and high contents of accessory minerals, mostly titanite and allanite, which is reflected in a clear distinction in aerogammaspectrometric maps due to high Th contents (Ferreira et al., 1991). It corresponds to the **Itapevi-type**, which makes up a main elongated body in the eastern part of Fig. 2 (the Itapevi pluton, ca. 39 km long), and a minor body next to the Caucaia Shear Zone. There is a wide variation of mafic content, from predominant felsic equigranular biotite granites to mafic inequigranular granodiorites. Strongly deformed porphyritic biotite granites that occur in the eastern part of Fig. 1 are of uncertain affinity, sharing features of the Itapevi and Ibiúna types.

Table 1
Summary of the hierarchy adopted for the syn-orogenic associations and types of the Agudos Grandes Batholith.

association	type	Predominant Composition
High-K calc-alkaline (HKCA)	Ibiúna (Ibiúna, Jurupará, Cotia plutons	porphyritic biotite-hornblende quartz monzonite to granodiorite, M = 10-15
	Tapiraí	porphyritic hornblende-biotite monzogranite, M = 8-10
	Rio Taquaral	porphyritic biotite-hornblende granodiorite
Itapevi	mafic Itapevi	inequigranular biotite granodiorite, M = 10-20
	felsic Itapevi	felsic equigranular biotite granite, M < 10
	porphyritic Itapevi	Porphyritic biotite quartz monzonite to granodiorite, M > 12
Turvo	Turvo	muscovite-biotite leucogranite, M < 5

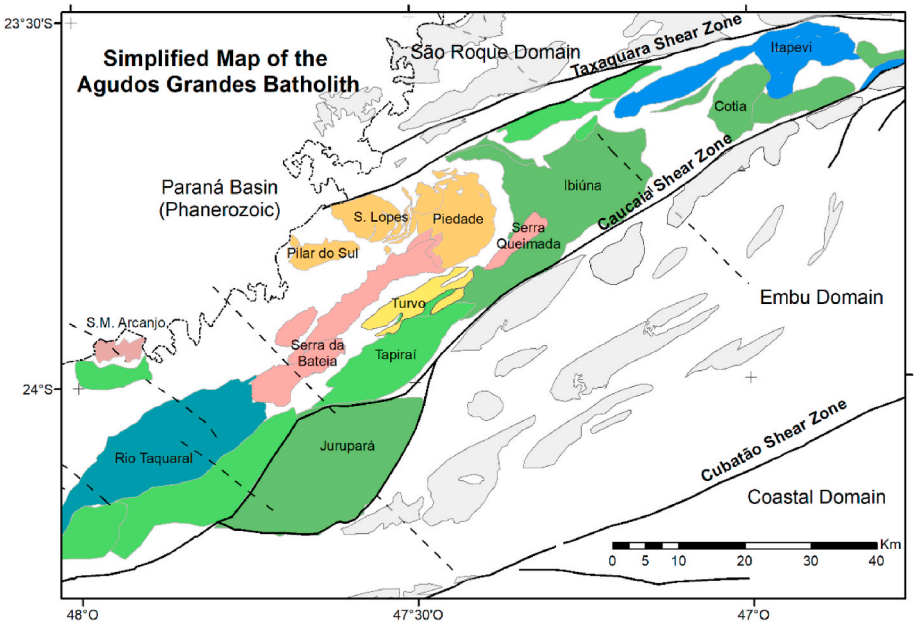

Fig. 2. Simplified map of the Agudos Grandes Batholith. Colors refer to the batholith granite associations (see text). Names refer to plutons referred in text. Other Neoproterozoic granites are shown in grey.

A third granite association corresponds to a (usually slightly foliated) muscovite-biotite leucogranite with local garnet and tourmaline-bearing facies, which makes up the Turvo pluton. At the borders of this pluton these leucogranites crosscut the Tapiraí and Ibiúna-type granites, indicating a younger emplacement.

3.2. Late and post-orogenic granitic magmatism

Late- and post-orogenic granitic magmatism of the eastern Agudos Grandes Batholith was the subject of previous geochronologic and petrologic research by Janasi et al. (2001) and Leite et al. (2006, 2007a, b).

Late-orogenic magmatism, dated at 605-600 Ma (Leite et al., 2007a) manifests as an array of subcircular, zoned plutons intrusive into metasupracrustal sequences of the Embu Complex and Votuverava Formation in the region of the Piedade and Pilar do Sul towns. Piedade is the most complex pluton, with a core of metaluminous porphyritic titanite-biotite granite enveloped by more evolved pink inequigranular biotite granite and an external ring of porphyritic peraluminous muscovite-biotite granite. Serra dos Lopes is dominated by inequigranular biotite granite, and the westernmost Pilar do Sul Pluton is formed by equi to inequigranular muscovite-biotite leucogranite with local hydrothermal effects that generated greisen and quartz veins.

Post-orogenic magmatism occurs as two sets of A-type granites. The small 585 Ma São Miguel Arcanjo Granite, partly covered by Phanerozoic sediments of the Paraná Basin, is a slightly foliated porphyritic hornblende-biotite K-feldspar-rich monzogranite with color index 8–10. The elongated ~565 Ma Serra da Bateia and Serra da Queimada plutons are dominated by a porphyritic biotite syenogranite with color index 7–8 and a distinctive magmatic foliation defined by the iso-orientation of tabular ~2–3 cm long alkali feldspar megacrysts (Janasi et al., 2001). We also included for comparison the post-orogenic Capão Bonito pluton, formed by coarse-grained, red biotite syenogranites with low color index (4–5); it is coeval with São Miguel Arcanjo (586 ± 3 Ma; Leite et al., 2007a,b), and occurs further west of the Agurdos Grandes Batholith, intruding the Três Córregos Batholith.

4. Methods

Whole-rock major and trace-element data (by XRF and solution-ICPMS, respectively), Sr–Nd isotope data (by TIMS and solution-ICPMS, respectively) and U–Pb dating by SHRIMP were obtained in laboratories of the Instituto de Geociências, Universidade de São Paulo, Brazil. In situ Pb isotope analyses in alkali feldspar crystals and additional U–Pb zircon dating were obtained at the Radiogenic Isotope Facility (RIF), University of Alberta, Edmonton, Canada using a Multicollector ICPMS Nu Plasma coupled to a 213 nm Nd:YAG laser system. Details of the analytical protocols of all methods employed are presented in Supplementary File 1.

5. Geochronology

Previous published work by Janasi et al. (2001) and Leite et al. (2007a) established the chronostratigraphy of the Agudos Grandes Batholith based on ID-TIMS U–Pb dating of zircon and monazite. The evolution of the batholith spanned at least 45 Myr; the age of the HKCA association that constitutes most of the batholith's volume was constrained by a U–Pb zircon age of 610 ± 2 Ma and is identical to that of minor biotite-muscovite leucogranites (Turvo Pluton) dated at 610 ± 1 Ma. The third type of "syn-orogenic" granites (Itapevi-type) remained undated so far. This "syn-orogenic" magmatism that formed ENE elongated plutons parallel to the batholith direction was followed by "late-orogenic" round-shaped plutons made up of biotite ± muscovite granites whose ages are slightly younger (605-600 Ma).

5.1. SHRIMP U–Pb zircon dating

For the present work, we additionally obtained U–Pb SHRIMP ages on zircon for three samples (Supplementary File 2). Two of these samples were previously dated by ID-TIMS by Janasi et al. (2001) and we chose to re-study them to check for consistency with our recent results for neighbor granites that have been obtained by SHRIMP, and also to investigate the presence of inherited zircon. A third sample is an augen-gneiss that is representative of the typical occurrences in the easternmost part of the batholith near the city of São Paulo, and is inferred to correspond to the Ibiúna-type granites strongly affected by strike-slip deformation.

Ibiúna-type hornblende-biotite monzogranite PD-526 was previously dated by Janasi et al. (2001) and yielded a precise age of 610 ± 2 Ma, based on two concordant zircon fractions, with other fractions strong effects of Pb loss and clear evidence of inheritance. Our new results yield a Concordia age of 607 ± 6 Ma, based on 9 out of 12 analyzed spots (Fig. 2), that is identical within error to the previous result. A single inherited core (spot 9.1) yields a Paleoproterozoic $^{207}Pb/^{206}Pb$ age (2156 ± 11 Ma) with 8% discordance. Two slightly younger results (spots 10.1 and 12.1 with ~600 Ma $^{238}Ub/^{206}Pb$ ages) were excluded due to higher (>10%) discordance.

Muscovite-biotite monzogranite sample PD-420 is from the external unit of the "late-orogenic" Piedade Pluton. Its age was estimated by Janasi et al. (2001) from a discordia traced from two zircon and one monazite fraction and yielded 605 ± 7 Ma. Evidence of inheritance and Pb loss was present in the other zircon and monazite fractions. Our new results yield a Concordia age of 608 ± 7 Ma, based on 9 concordant spots (Fig. 3), that is identical within error to the previous age. Three inherited cores yielded $^{207}Pb/^{206}Pb$ ages in the range 1.18–1.36 Ga, with the most concordant fraction yielding a more precise age of 1242 ± 27 Ma. It is remarkable that this is identical to the $^{207}Pb/^{206}Pb$ age of a non-magnetic population of large zircon crystals dated by Janasi et al. (2001) at 1253 ± 5 Ma.

Hornblende-biotite "augen-gneiss" B-1 outcrops at the campus of the University of São Paulo, and was referred to as the "Butantã" gneiss in previous literature (Coutinho, 1972); we interpret these rocks as strongly deformed equivalents of the Ibiúna-type monzogranites, in view of compositional similarities and field relationships. A Concordia age of 621 ± 4 Ma was obtained from 12 concordant spots (Fig. 3). Three spots with large (1.6–0.6%) proportion of common ^{206}Pb or large errors in $^{207}Pb/^{235}U$ were excluded from regression; if included, the resulting age would be similar (620 ± 3 Ma). A single inherited core was analyzed, but the data is strongly discordant; anchored at the magmatic age of 621 Ma, it yields an upper intercept of ~2.0 Ga.

5.2. LA-MC-ICPMS zircon dating

Two samples of felsic Itapevi-type biotite granites were dated by LA-ICPMS (U–Pb in zircon) and yield identical Concordia ages of 608 ± 5 Ma (PD-2406) and 607 ± 5 Ma (PD-2419) (Supplementary File 3; Fig. 4). Inherited cores are present in both samples. Four inherited cores dated in sample PD-2406 belong to a single population yielding an upper intercept at 1691 ± 31 Ma; two populations of inherited crystals were identified in sample PD-2419, one defined by a single concordant crystal at 2095 ± 17 Ma, and a second by two crystals with upper intercept at 1786 ± 26 Ma.

6. Elemental geochemistry

6.1. Classification diagrams

All whole-rock elemental geochemistry data obtained for the syn-orogenic granitic rocks of the Agudos Grandes are presented in Supplementary File 4. The granitic rocks were classified using the conventional diagrams summarized by Frost et al. (2001) (Fig. 5) that clearly

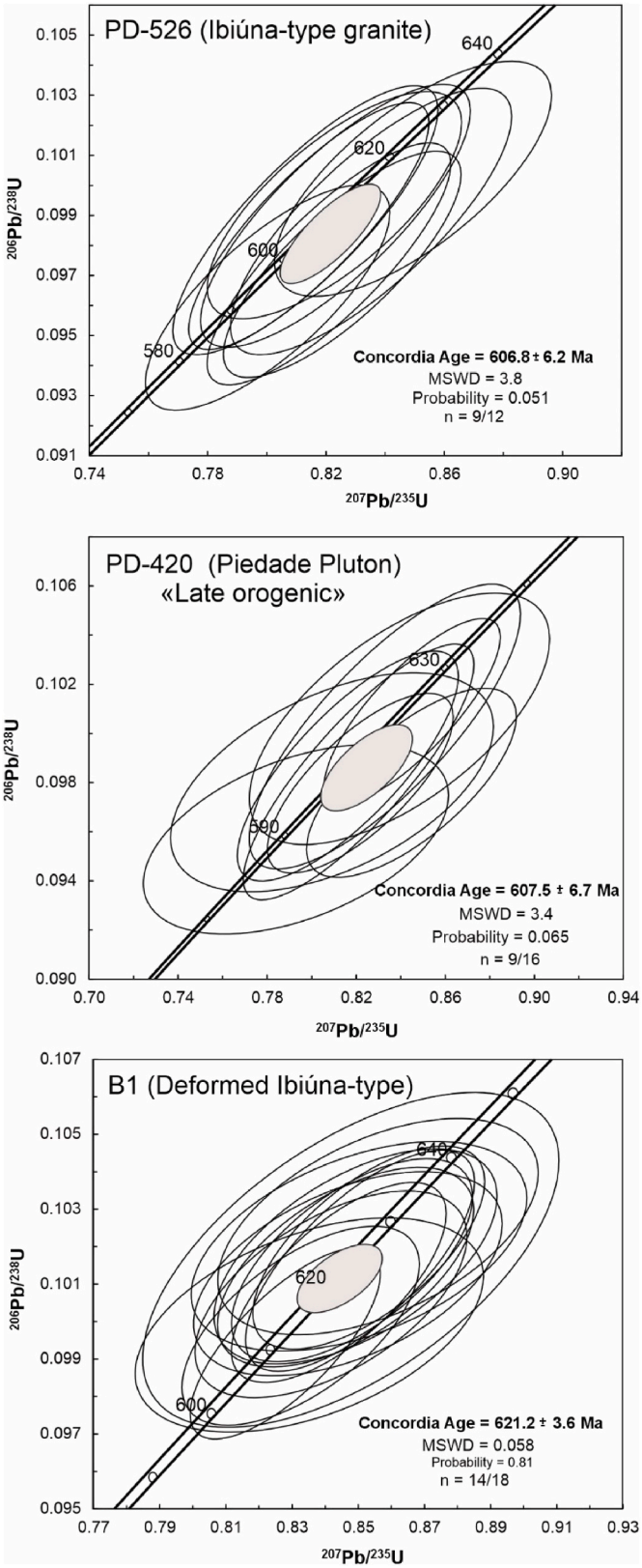

Fig. 3. Concordia diagrams showing zircon U–Pb analyses by SHRIMP used to obtain the ages of granites and augen-gneiss form the Agudos Grandes.

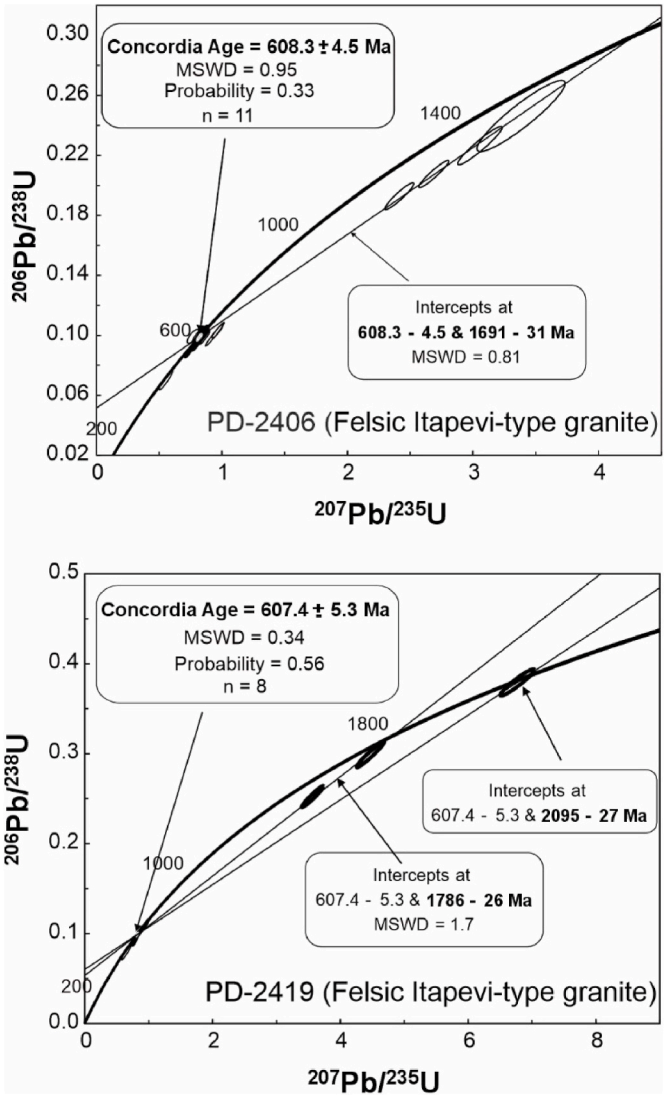

Fig. 4. Concordia diagrams showing zircon U–Pb analyses by LA-MC-ICPMS used to obtain the ages of granites Itapevi-type granites.

distinguish the main associations. All rocks with a few exceptions fall in the alkali-calcic field; the HKCA association and the mafic Itapevi type are metaluminous; the felsic granites fall in the limit between the metaluminous and peraluminous fields, with the exception of the Turvo leucogranite, which is markedly peraluminous with A/CNK = 1.08–1.13. Two samples of Itapevi porphyritic biotite granite are also peraluminous. The N/K (molar Na_2O/K_2O) and F/FM (molar $FeO_t/(FeO_t + MgO)$ ratios distinguish the HKCA association and its fractionated equigranular granite, which are frankly magnesian, from the Itapevi association, which has lower N/K and tends to be ferroan, especially in the more differentiated compositions. It is interesting that the porphyritic biotite granites are magnesian, but their behavior is intermediate between the HKCA and the Itapevi associations.

6.2. *Major and trace element variations*

Binary chemical variation diagrams using silica as the fractionation index are shown in Figs. 6 and 7. A relatively wide silica range is shown by the HKCA and Itapevi associations, and they follow different trends in several diagrams. In terms of major oxides, the main contrasts are shown by Fe, Mg, Na and K, with the HKCA association (including the Jurupará equigranular granites that correspond to its felsic differentiates)

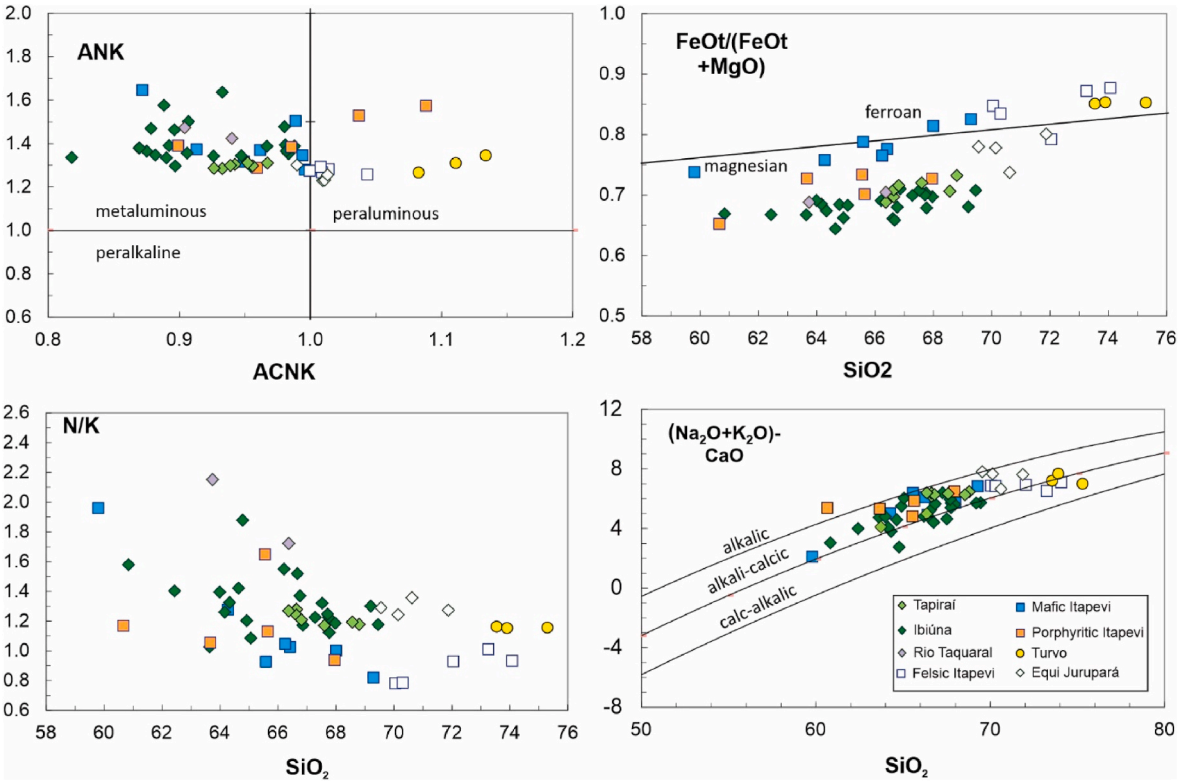

Fig. 5. Classification diagrams used to determine the geochemical affinities of syn-orogenic granites from the Agudos Grandes batholith. N/K = molar Na_2O/K_2O; ANK = molar $Al_2O_3/(Na_2O + K_2O)$; ACNK = molar $Al_2O_3/(CaO + Na_2O + K_2O)$. Fields are from Maniar and Piccoli (1989) (diagram (a)) and Frost et al. (2001) (diagrams (b) and (d)). Shapes of symbols refer to Ibiúna (diamonds), Itapevi (squares) and Turvo (circle) associations.

showing higher Mg and Na and lower Fe and K, a feature already apparent in the classification diagrams previously presented. Trace-elements further contrast these two associations, with the Itapevi association defining trends with higher HFSE (Zr, Nb), LREE (e.g., Ce), Th, U and Rb, and lower Sr and Ba.

Among the felsic rocks (>70 wt% SiO_2), the Turvo leucogranite is clearly distinguished by high Al contents, reflecting its peraluminous character, but also by lower Fe, Ti and Zr and higher Na, Mn and, as common in peraluminous granites, also P.

Among the three types of granitoids from the HKCA association, the Ibiúna type is characterized by higher Mg and Fe and slightly higher **mg#**. Rio Taquaral type is characteristically richer in Na and Al and poorer in K and Ti. Apart from slightly lower **mg#**, Tapiraí is only distinguished from the Ibiúna type by slightly lower CaO; however, it tends to be a little richer in most incompatible trace-elements, e.g., Ba, Sr, Zr, Ce, Th and Nb. On the contrary, Rio Taquaral is poorer in the same trace-elements, except for Sr, resulting in the lowest Ba/Sr ratios in the HKCA association.

The porphyritic biotite granites of uncertain connection have some features in common with the Tapiraí type. The behavior of many trace-elements is intermediate between the HKCA and Itapevi associations (e.g., Zr, Rb, Th, Ce); however, Ba and Sr contents are even higher than those of the HKCA granitoids.

6.3. Rare-earth patterns

REE patterns normalized to chondrite (Fig. 7) are fractionated [$(La/Yb_N) = 22–42$] with negative Eu anomalies varying from discreet in the Ibiúna association to well-developed in the other granites. Within the Ibiúna association, the Rio Taquaral sample is distinguished by lower fractionation [$(La/Yb)_N = 17$] and near absence of Eu anomaly [$(Eu/Eu^*)_N = 0.89$] compared to Tapiraí [$(La/Yb)_N = 50–60$; $(Eu/Eu^*)_N = 0.75–0.85$]; although variable, fractionation of the REE patterns of the Ibiúna-type are intermediate [average $(La/Yb)_N = 30$], whereas Eu anomalies are similar to Tapiraí [average $(Eu/Eu^*)_N = 0.79$].

Typical REE patterns of mafic and porphyritic Itapevi are strongly fractionated [$(La/Yb)_N = 45–95$] with moderate negative Eu anomalies [$(Eu/Eu^*)_N = 0.62–0.79$]; sample PD268 is an exception with less fractionated pattern and a well-developed Eu anomaly (Fig. 8).

Felsic Itapevi samples also show variably fractionated patterns, but characteristically have very negative Eu anomalies [$(Eu/Eu^*)_N = 0.3–0.4$]. In contrast, equigranular Jurupará shows strongly fractionated patterns with weak Eu anomalies, whereas the Turvo leucogranite has unfractionated REE patterns [$(La/Yb)_N = 6–19$] with low LREE and well-developed negative Eu anomalies [$(Eu/Eu^*)_N = 0.5$] typical of very evolved granites.

7. Isotope geochemistry

7.1. Whole-rock Sr–Nd isotope ratios

Whole-rock Sr and Nd isotope ratios were obtained for representative samples of the syn-orogenic granites, and are plotted in an $^{87}Sr/^{86}Sr(t)$ x $\varepsilon Nd(t)$ diagram in Fig. 8; analytical results are presented in Supplementary File 5, together with a compilation of previously published data used in the following.

Among the studied syn-orogenic granites, a clear distinction can be observed, with the HKCA granites showing strongly negative $\varepsilon Nd(t)$ (−14 to −18) and $^{87}Sr/^{86}Sr(t) = 0.710–0.711$; the Itapevi-type granites, represented by three felsic samples, have even more negative $\varepsilon Nd(t)$ (−19 to −20) and more radiogenic Sr ($^{87}Sr/^{86}Sr(t) = 0.712–0.713$), while the peraluminous Turvo leucogranite combines less negative $\varepsilon Nd(t)$ (~-14) and radiogenic Sr ($^{87}Sr/^{86}Sr(t) = 0.717$).

We included in Fig. 9 the results reported in our previous work for the late- and post-orogenic plutons of the Agudos Grandes Batholith (Leite et al., 2006, 2007b). The late-orogenic plutons define a

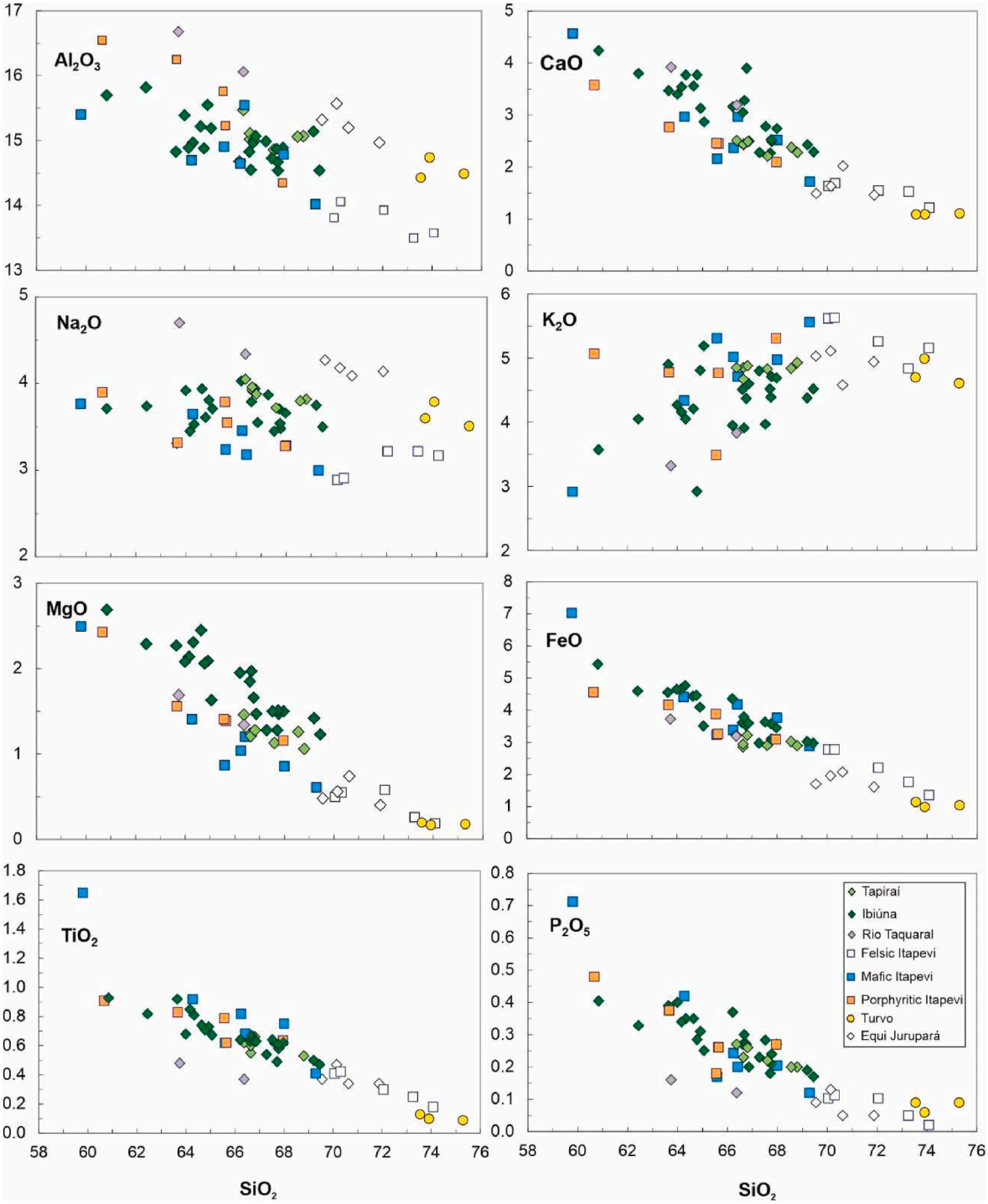

Fig. 6. Major and minor oxide variation diagrams for the syn-orogenic granites from Agudos Grandes Batholith using SiO_2 as differentiation index. Shapes of symbols refer to Ibiúna (diamonds), Itapevi (squares) and Turvo (circle) associations.

continuous trend between more primitive metaluminous granites from the Piedade Pluton (with the extreme given by a dike with εNd(t) = −12.6 and $^{87}Sr/^{86}Sr(t)$ = 0.708) and slightly peraluminous granites from the Pilar do Sul at εNd(t) = −16.2 and $^{87}Sr/^{86}Sr(t)$ = 0.715 interpreted as a result of contamination with crustal melts similar to the Turvo leucogranite. The Sr–Nd isotope signature of the ~585 Ma post-orogenic São Miguel Arcanjo and Capão Bonito seem to follow the trend of the late-orogenic granites reaching even higher $^{87}Sr/^{86}Sr(t)$ (0.718 in Capão Bonito). The ~565 Ma post-orogenic Serra da Bateia/Serra da Queimada granites show less negative εNd(t) (−10 to −11.5); $^{87}Sr/^{86}Sr(t)$ is ~0.712 in the two samples with lower Rb/Sr, while the other two samples have high $^{87}Rb/^{86}Sr$ (6.6–9.7), and as such their higher $^{87}Sr/^{86}Sr(t)$ (0.716–0.718) carry a large uncertainty.

7.2. K-feldspar Pb–Pb isotope ratios

Pb–Pb isotope ratios are excellent markers of magma sources, but very few published data exist for the Neoproterozoic granites from SE Brazil. We obtained in situ Pb–Pb ratios of K-feldspar directly on polished rock slabs by LA-ICP-MS of selected samples from the Agudos

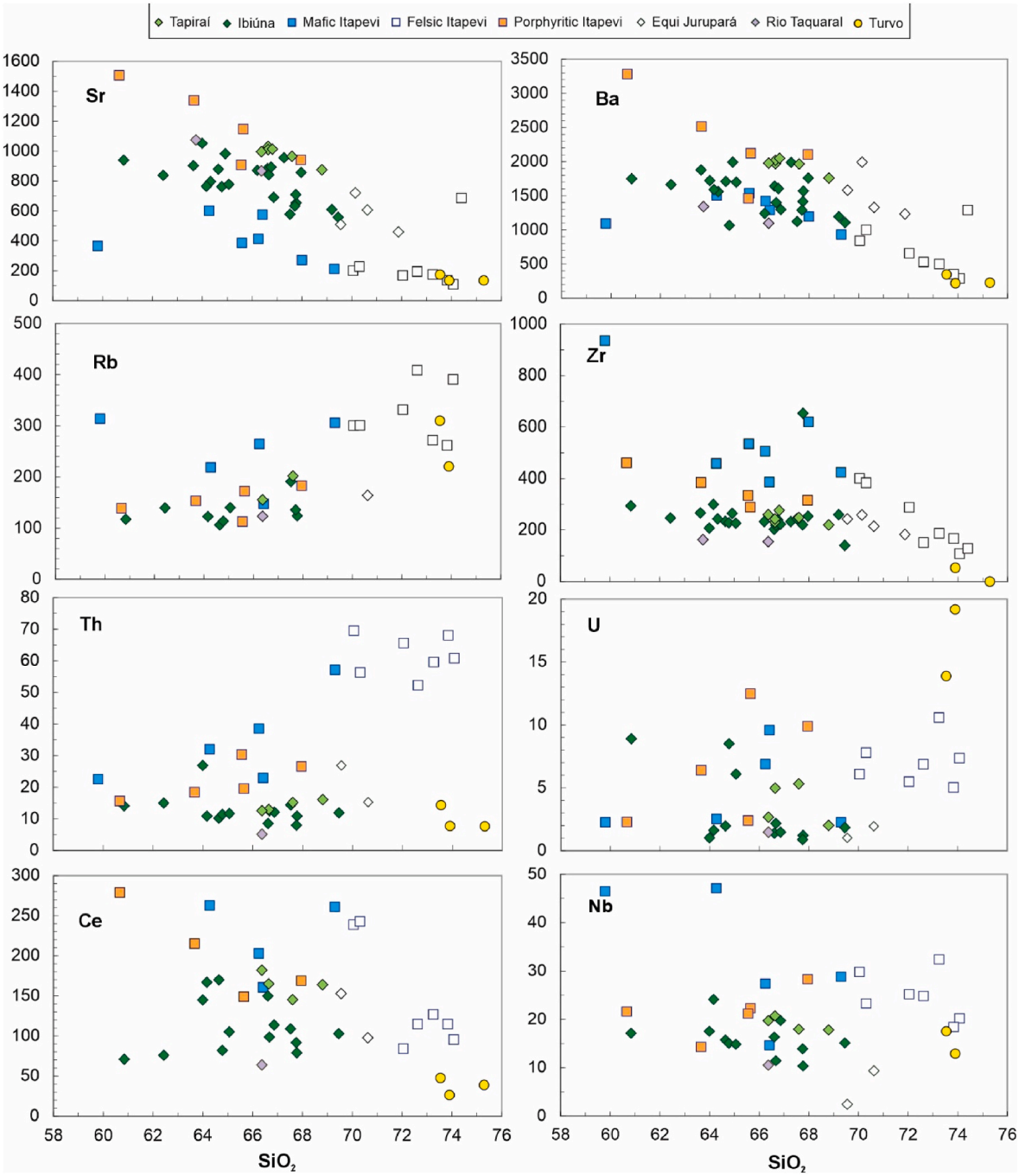

Fig. 7. Trace-element variation diagrams for the syn-orogenic granites from Agudos Grandes Batholith using SiO2 as differentiation index. Shapes of symbols refer to Ibiúna (diamonds), Itapevi (squares) and Turvo (circle) associations.

Grandes Batholith (see Methods). We also obtained results from representative samples of late- and post-orogenic granites previously analyzed for Sr and Nd isotopes to acquire a complete picture of the time evolution of magma sources that contributed to the batholith (see Supplementary File 6).

Significant contrasts exist among the syn-orogenic granites (Fig. 9). The HKCA and the Itapevi sample are characterized by low $^{206}Pb/^{204}Pb$ ratios (16.3–16.7). Within this group, the Tapiraí-type is slightly more radiogenic; higher $^{208}Pb/^{204}Pb$ (over the lower-crust evolution curve) distinguishes the Itapevi sample. The Turvo peraluminous leucogranite is significantly more radiogenic (e.g., $^{206}Pb/^{204}Pb = 17.5$). The late-orogenic samples are from the Piedade (one each from the metaluminous core and peraluminous border units of Leite et al., 2006) and Pilar do Sul plutons, and their Pb isotope signatures are intermediate between the HKCA and Turvo granites (e.g., $^{206}Pb/^{204}Pb = 17.1$). Both syn-orogenic and late-orogenic granites are characterized by high μ ($=^{238}U/^{204}Pb$), aligning slightly below a Pb growth curve with μ~10; the HKCA and Itapevi syn-orogenic granites derive from a source with higher Pb model age relative to the late-orogenic granites (see discussion).

Samples from the ~580 Ma post-orogenic A-type São Miguel Arcanjo and Capão Bonito plutons have $^{206}Pb/^{204}Pb$ ratios slightly higher than the late-orogenic granites (17.2–17.3) and are distinguished by higher $^{208}Pb/^{206}Pb$. The sample from the youngest ~565 Ma post-orogenic A-type Serra da Bateia granite is the more radiogenic of the whole set, with $^{206}Pb/^{204}Pb = 17.7$. The Capão Bonito and Serra da Bateia granites have

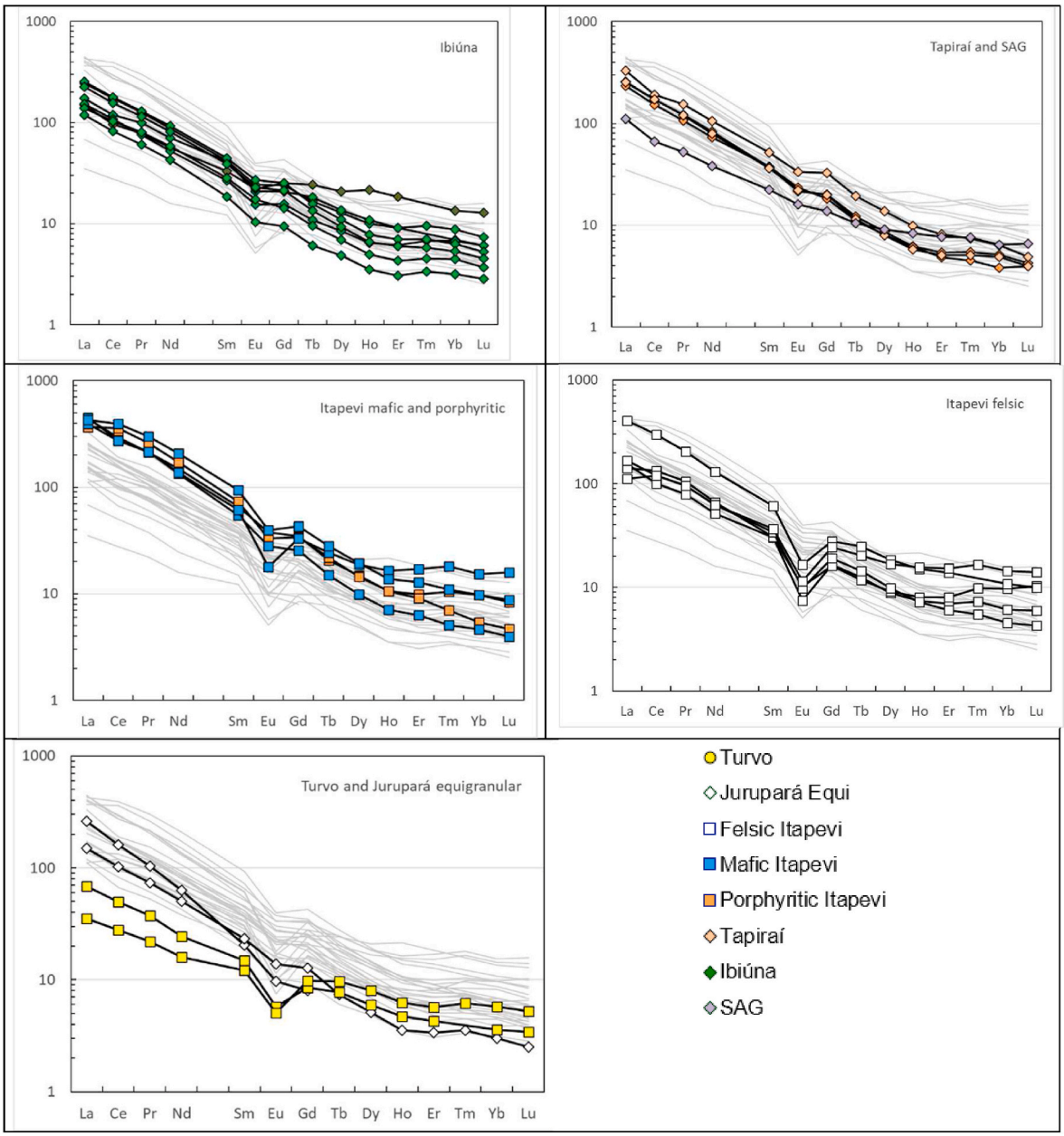

Fig. 8. C1-chondrite-normalized (values from Mcdonough and Sun, 1995) REE patterns of syn-orogenic granites from the Agudos Grandes Batholith. Shapes of symbols refer to Ibiúna (diamonds), Itapevi (squares) and Turvo (circle) associations.

μ values close to the Stacey and Kramers (1975) Pb growth curve, lower than the other granites from the batholith.

8. Discussion

8.1. Petrogenesis of the syn-orogenic magmatism: inferences from whole-rock geochemistry

The **HKCA metaluminous hornblende-biotite granitoids** that make up most of the batholith have relatively high (~12–15) color indices and intermediate SiO_2 contents (64–68 wt%); they are akin to I-type granites, whose origin is still a matter of much debate (Clemens et al., 2011; Castro, 2014; Collins et al., 2016). As experimental products of crustal melting at realistic temperatures (<900 °C) are typically more silica-rich (and Mg, Fe-poor) than these granites, it is often admitted that they have a mantle component (e.g., Moyen et al., 2021). It is well-known, however, that granite composition may not correspond to that of a melt, as it may carry significant proportions of source-related solid components (restites, Chappell et al., 1987; peritectic minerals, Clemens et al., 2011; partly assimilated infertile mafic material; Carvalho et al., 2017), or may have a cumulate component (Barnes et al., 2020). Enclaves are important evidence of all such processes, and the only type of enclave found in the Agudos Grandes HKCA are rounded cm-sized mafic/intermediate enclaves with grain-size smaller than the matrix of the host rock. Although these might be taken as evidence of a mantle contribution, they are very scarce, and larger mafic bodies are also very uncommon in the batholith.

Rhyolite-MELTS equilibrium crystallization modeling the whole-rock composition of a typical Agudos Grandes HKCA granite at reasonable melt water contents and at pressures consistent with the emplacement depths (e.g., 4 wt%; 300–500 MPa) yields very high *liquidus* temperatures (~1050 °C), but the amount of liquid remains very high (>80 wt%) down to ~850 °C, when plagioclase begins to crystallize. Recent work admits that granite melts equilibrate in thick mush-

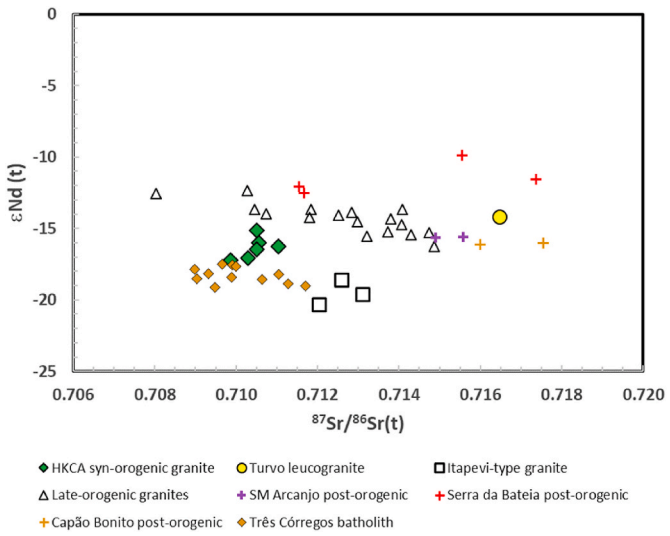

Fig. 9. $^{87}Sr/^{86}Sr(t)$ x εNd(t) variation diagram for granites from the Agudos Grandes Batholith. HKCA, Itapevi ad Turvo from this work; data for late-orogenic and post-orogenic granites from Leite et al. (2007b). Data from the Três Córregos Batholith (from Prazeres Filho et al., 2003) are plotted for comparison. Shapes of symbols refer to Ibiúna (diamonds), Itapevi (squares), Turvo (circle), late-orogenic (triangle) and post-orogenic (crosses) associations.

dominated crustal hot zones and are typically multiply-saturated with a hornblende gabbronorite assemblage (Blundy, 2022). Assuming this, the mafic mineral crystallized at high temperature (two pyroxenes + spinel) might be interpreted as excess solid components residing in a more felsic melt. Zircon saturation temperatures of the Ibiúna and Tapiraí HKCA granites (calculated using the Watson and Harrison, 1983 calibration) are tightly concentrated in the 780–810 °C range; at whole-rock 64–68 wt% SiO_2, a granitic melt is not expected to be zircon-saturated (Siégel et al., 2018) and these would be therefore *subliquidus* temperatures. On the other hand, P_2O_5 contents varying between 0.15 and 0.40 wt% correspond to very high apatite saturation temperatures (900–1000 °C using the Harrison and Watson, 1984 calibration), and would imply either that these are indeed the *liquidus* temperatures or that apatite is a cumulate or restite phase.

Typical features of the Agudos Grandes HKCA granites are fractionated REE patterns with small negative Eu anomalies and high Sr/Y (~60), mostly reflecting high Sr contents (600–1000; average 850 ppm). High Sr/Y is often interpreted as indicative of magma equilibration at high crustal pressures where garnet is stabilized at the expense of plagioclase (Gromet and Silver, 1987; Whalen and Hildebrand, 2019) and was proposed as a proxy for crustal thickness (Chapman et al., 2015) during magma evolution. However, plagioclase accumulation may increase the Sr and Eu contents (Brackman and Schwartz, 2022), so that the original Sr/Y of granitic melts would be more appropriately estimated from the composition of minerals. We are currently undertaking such mineral-scale studies, and these appear to confirm that relatively high Sr/Y is indeed a feature of the magmas that formed the Agudos Grandes HKCA melts. We used the equations by Hu et al. (2017) for collisional belts and obtained high values (66 km) for crustal thickness using the median of Sr/Y (= 57) and still high, but lower (58 km), using the $(La/Yb)_N$ ratio (median = 38), that is not affected by plagioclase accumulation.

The three variants of HKCA granitoids (Ibiúna, Tapiraí and Rio Taquaral) share most compositional characteristics, and as such are inferred to have a common origin. Tapiraí and Rio Taquaral show opposite behavior in a series of elements as compared to the most voluminous Ibiúna type: Rio Taquaral is distinguished by higher Na/K, lower Ba, Ti, P, LREE and Zr (at a given SiO_2 content) and less fractionated REE patterns, reflecting either differences in source or, most likely, in conditions of melting (e.g., lower T, higher H_2O).

The Jurupará equigranular biotite granites are felsic rocks that occur in direct association with the Ibiúna-type HKCA in the homonymous pluton, and their composition is consistent with that of felsic differentiates from the predominant intermediate hornblende-biotite granitoids.

The **Itapevi** association spreads a wide range of silica contents (60–75 wt% SiO_2); granites with >70 wt% SiO_2, described as "felsic Itapevi", are slightly peraluminous, and the more mafic granites, although metaluminous, rarely show hornblende (biotite is the main mafic mineral, and titanite the Ca-rich phase). It is distinguished by remarkably high contents of some incompatible elements (Th, LREE, Zr, Nb), reflected in the abundance in accessory phases that carry them (mostly allanite and titanite), and by consistently lower Sr contents and negative Eu anomalies. These features are interpreted as reflecting a distinct source, with residual plagioclase, and melting at higher temperatures, to account for the higher contents of HFSE, LREE, Th and U. Equilibration at lower depths (lower Sr/Y; residual plagioclase) and higher T are features of A-type granites, but the Itapevi granites differ from these by their continuous (not bimodal) compositional variation, deformed character and contemporaneity with calc-alkaline magmatism. The abundance of mafic-rich compositions is not consistent with generation by crustal anatexis; unless they carry a large restitic component, these granites must have some contribution from a mafic (mantle-derived?) component.

It is remarkable that a suite of **"porphyritic biotite granites"** occurs in areas where the Ibiúna (HKCA) and Itapevi granites are in close contact, since they have many geochemical characteristics that are intermediate between these two suites (except, for instance, for Sr contents that are even higher than Ibiúna). In general terms, they could be evidence of interaction between magmas (or sources) from these two suites.

Among the three major types of syn-orogenic granites from the Agudos Grandes batholith, the subordinate **Turvo** (tourmaline)-biotite-muscovite leucogranite is the most evidently associated with crustal anatexis, given its high silica content, peraluminous character and geochemical and isotopic signature similar to those of S-type granites. It may therefore be used as reference for a typical product of low-temperature (~700 °C; zircon saturation temperature from Watson and Harrison, 1983 calibration) crust-derived melt in the batholith.

8.2. Inferences from isotope geochemistry: source evolution from syn-to post-orogenic magmatism in the Agudos Grandes Batholith

Strongly negative εNd(t) (−13 to −20) and high (but restricted) $^{87}Sr/^{86}Sr(t)$ (0.710–0.717) are shown by all syn-orogenic granitoids from the Agudos Grandes Batholith, implying a predominant contribution of sources with long crustal residence. Each of the three groups of syn-orogenic granites shows a specific Sr–Nd isotope signature: HKCA with the lowest $^{87}Sr/^{86}Sr(t)$ (0.709–0.711) and intermediate (−15 to −17) εNd(t), Itapevi with higher $^{87}Sr/^{86}Sr(t)$ (0.712–0.713) and more negative εNd(t) (−19 to −20) and the single sample of Turvo leucogranite with the highest $^{87}Sr/^{86}Sr(t)$ (0.717) and less negative εNd(t) (−14). The εNd(t) contrast between Itapevi and Turvo (the latter interpreted as a typical product of low-temperature crustal anatexis) implies that a source with older crustal residence was involved in the genesis of Itapevi.

When the late-orogenic plutons (studied by Leite et al., 2006, 2007a, b) are considered, it is observed that the continuous trend from metaluminous biotite granites of the Piedade pluton (εNd(t)- 12, $^{87}Sr/^{86}Sr(t)$ = 0.710) to peraluminous leucogranites of the Pilar do Sul pluton (−16 and 0.715), respectively, extends to values close to the syn-orogenic Turvo leucogranite, and has less negative εNd(t) than both the HKCA and Itapevi syn-orogenic granites. This suggests that the crustal sources that were mobilized in the late-orogenic period have similar crustal residence to those previously melted to generate the low-temperature Turvo granites. The age differences involved are very small, almost

unresolvable within the uncertainties of zircon U–Pb SHRIMP dating (see Janasi et al., 2001; Leite et al., 2007a), but we consider this an evidence of a thermal anomaly rising in a stratified crust with older sources residing in the deepest levels. The εNd(t) of the post-orogenic A-type granites are also indicative of a source with shorter crustal residence (when compared to HKCA and Itapevi), with the youngest ~565 Ma Serra da Bateia granite showing the least negative values (−10).

The Pb isotope data presented in this contribution are the first reported for the Agudos Grandes Batholith, and allow some important constraints on the sources of granite magmatism. The $^{207}Pb/^{206}Pb$ ratio reflects the age of the sources, and our results confirm that the HKCA and Itapevi granites derive from sources that are older than those that generated Turvo and the late-orogenic granites ($^{207}Pb/^{206}Pb$ = 0.94–0.96 × 0.89–0.91). We included the Sr-Nd-Pb data reported by Prazeres Filho et al. (2003) for HKCA granites from the neighbor Três Córregos Batholith, also intrusive into the Apiaí-São Roque Domain of the Ribeira Fold Belt; their isotope signature is similar to those of similar granites from Agudos Grandes. Indeed, a clear negative correlation between $^{207}Pb/^{206}Pb$ and εNd(t) can be observed when the whole dataset is considered (Fig. 11), with the post-orogenic A-type Serra da Bateia granite and the Três Córregos HKCA granites defining the "youngest" (least negative εNd(t), lowest $^{207}Pb/^{206}Pb$) and "oldest" poles, respectively.

Further information can be extracted from other Pb/Pb ratios. ^{208}Pb is a daughter isotope of ^{232}Th, and therefore the $^{208}Pb/^{206}Pb$ ratio is a direct reflection of the $^{232}Th/^{238}U$ ratio (κ) of the source. A negative correlation between $^{208}Pb/^{206}Pb$ and $^{207}Pb/^{206}Pb$ is evident for the whole set of Agudos Grandes granites (Fig. 10c), showing that as the sources get younger they also have lower Th/U. The Itapevi sample departs from the general trend showing a higher κ value (4.6) typical of an old lower crustal source (with U depletion relative to Th; e.g., Halla, 2018), but its uranogenic lead is high (μ = 9.7), requiring a high U/Pb source, which is therefore distinct from the model lower crust of Zartman and Doe (1981). A high Th/U source is also suggested by the trace-element signature of the entire Itapevi association and its gamma-spectrometric signature.

K-feldspar crystals are considered to preserve the most recent resetting event of their host rocks, with Pb model ages typically interpreted as representing the point at which radiogenic ingrowth ceased. Three distinct groups can be identified based on Pb model ages (calculated at the Stacey-Kramers evolution curve): syn-orogenic HKCA and Itapevi granites yield Mesoproterozoic model ages ranging from 1250 to 1410 Ma; late-orogenic granites and the ~580 Ma São Miguel Arcanjo and Capão Bonito post-orogenic granites have Pb model ages around 1000 Ma; and the youngest Serra da Bateia granite yields a considerably lower Pb model age of 676 Ma. The only exception to this grouping is the Turvo granite, which, despite belonging to the oldest syn-orogenic group, yields a model age of 830 Ma. If all granite samples are considered together, an isochron yields an age close to 1.8 Ga (Fig. 11b).

When considered alongside Sr and Nd isotopes, the thoriogenic Pb data leads to some additional conclusions. The syn-orogenic magmatism appears to have recycled crustal reservoirs that have undergone extensive previous reworking. These reservoirs exhibit $^{87}Sr/^{86}Sr$ (~0.710), εNdt (−16 to −20), and κ values (~4), which indicate delayed radiogenic ingrowth due to the loss of Rb and U by previous melt extractions. It seems that these reservoirs experienced a major disruptive event

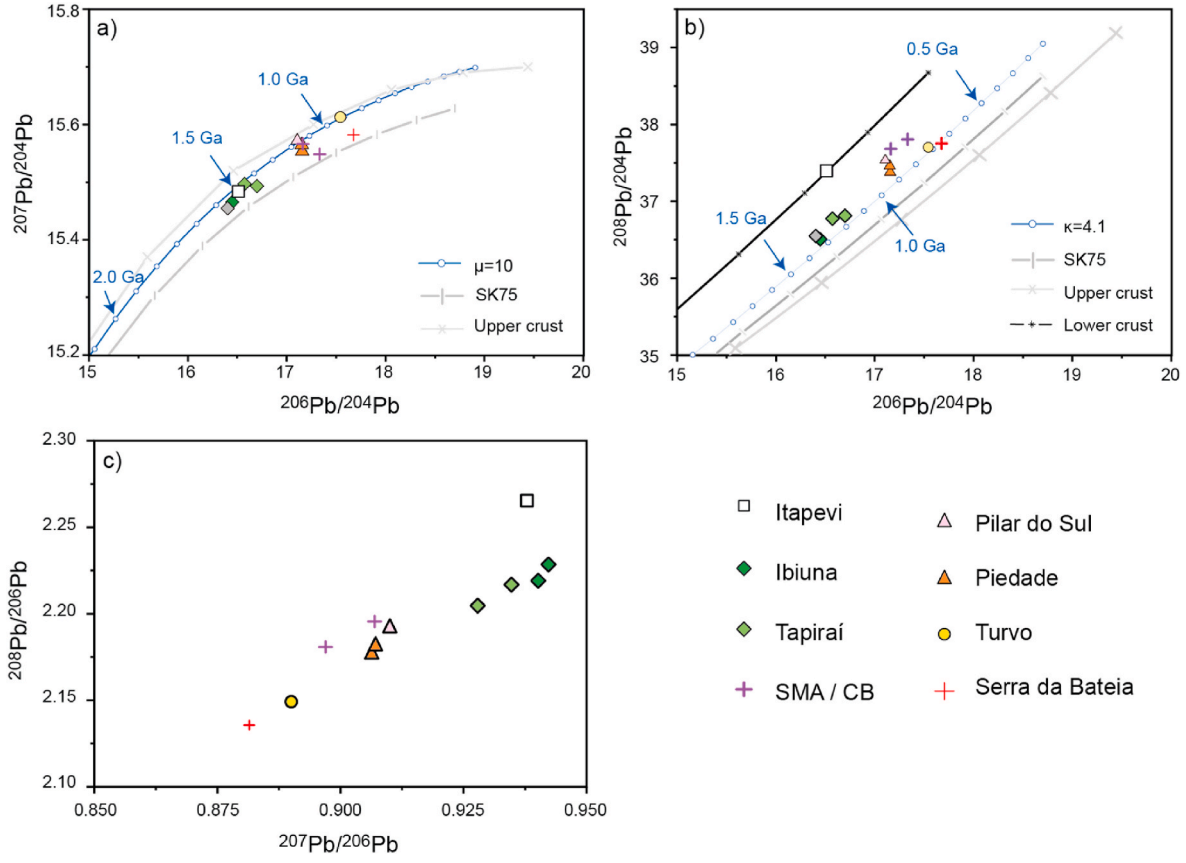

Fig. 10. K-feldspar Pb–Pb isotope diagrams. a) Uranogenic Pb and evolutionary lines with different μ values, blue arrows mark ages spaced at 100 Ma intervals for a curve with μ = 10 (μ = $^{238}U/^{204}Pb$); b) Thoriogenic Pb and evolutionary lines for different reservoirs according to Stacey and Kramers (1975) (SK75) and Zartman and Doe (1981), with the blue line marking the evolution of a reservoir under k = 4.1 (k = $^{232}Th/^{208}U$), with ages marked as blue arrows spaced at 100 Ma intervals. c) ^{208}Pb versus ^{207}Pb normalized by ^{206}Pb showing a tendency for thoriogenic Pb to increase with increasing age of the reservoir sampled by the granitic melts. Shapes of symbols refer to Ibiúna (diamonds), Itapevi (squares), Turvo (circle), late-orogenic (triangle) and post-orogenic (crosses) associations.

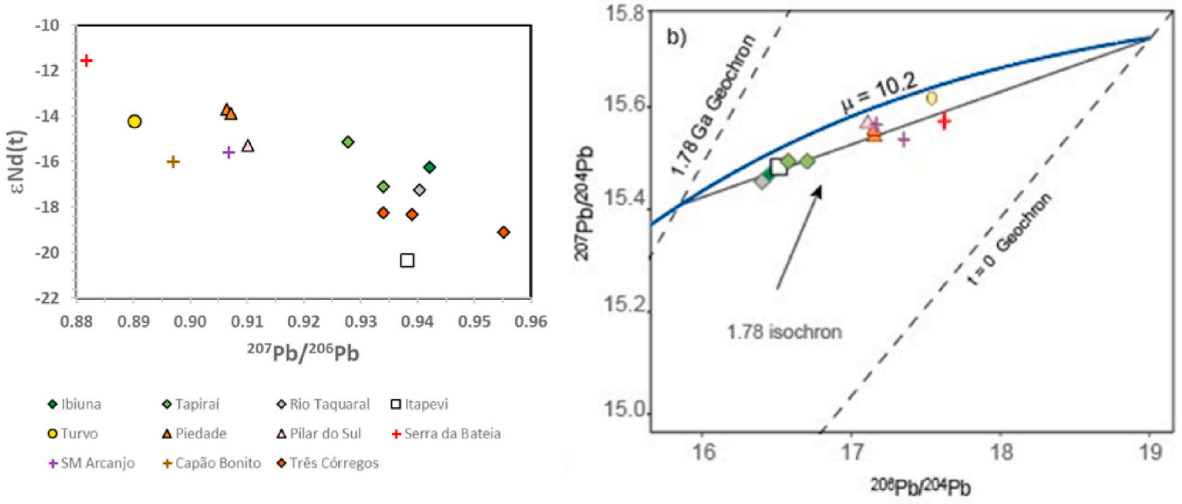

Fig. 11. Inferences from Pb and Nd isotopes. a) $^{207}Pb/^{206}Pb$ versus εNd(t); b) Spread of samples along a 1.78 Ga isochron (calculated with IsoplotR; Vermeesch, 2018) for a high-μ reservoir. Shapes of symbols refer to Ibiúna (diamonds), Itapevi (squares), Turvo (circle), late-orogenic (triangle) and post-orogenic (crosses) associations.

around 1380 Ma (the average of the two-stage Pb model ages), resulting in the last resetting of the Pb isotope system and potentially further accentuating Rb and U losses.

The isotope signatures of late- and post-orogenic granites indicate the participation of a more radiogenic crust, leading to elevated $^{87}Sr/^{86}Sr$ and μ, as well as reduced κ values in comparison with the syn-orogenic group. Such crustal reservoir also exhibits higher εNd(t) values (−11 to −15), younger Pb model ages (around 1000 Ma), and more radiogenic $^{87}Sr/^{86}Sr$ ratios. The combined isotope signatures of these granites is consistent with the involvement of younger and less depleted crust.

As a further argument consistent with the conclusions on the sources of granitic magmas presented here, we notice that the scarce data on the ages of inherited zircon indicate a contribution form older sources for the syn-orogenic HKCA (2.2 Ga in the Ibiúna sample; ~2.0 Ga in the augen-gneiss B-1) and Itapevi (1.7–2.1 Ga in the two samples dated here) and younger sources for the late-orogenic granites, as exemplified by the PD-420 Piedade sample (1.2–1.4 Ga; see also Janasi et al., 2001 for a few further data on zircon inheritance).

9. Tectonic implications

Our elemental and isotope data imply that a change in the magma sources occurred in a short time interval between the (main) syn-orogenic HKCA and Itapevi-type granites and the late-orogenic Piedade, Serra dos Lopes and Pilar do Sul plutons (~620-600 Ma). The sources of the older, "syn-orogenic" magmatism are inferred to have greater crustal residence (as shown by the Nd and Pb isotope signatures) and to be located at deeper levels of a thickened crust (as indicated by high Sr/Y ratios). As recently demonstrated by Campanha et al. (2019), the Agudos Grandes Batholith intrudes the contact between two distinct stratigraphic units: the Votuverava Group and the Embu Complex. The western, low-metamorphic grade Votuverava Group, is inferred to have a depositional age ~1.4–1.3 Ga based on U–Pb dating of amphibolites, whereas the Embu Group metasediments were deposited at ~0.97–0.85 Ga (Campanha et al., 2019). Importantly, provenance studies show contrasted sedimentary sources, with the Embu Complex recording a main age group of detrital zircon with 1.4-1.0 Ga and a minor group around 2.0–1.8 Ga, whereas the Votuverava Group is similar to other sedimentary units of the Ribeira Belt in the Apiaí and São Roque domains, with a strong peak at 2.2–2.0 Ga (cf. Henrique-Pinto et al., 2015). Both units show important signals of a metamorphic event at ~0.85–0.75 Ga event, which led Campanha et al. (2019) to infer that this is the age of juxtaposition of these units.

In such scenario, our data are suggestive that the syn- and late-orogenic granites of the Agudos Grandes Batholith equilibrated in a crust that was previously thickened (either during the ~0.85–0.75 collision or just before their generation). The initial and more voluminous magmas of HKCA character generated in a lower crust hot zone made up of older rocks of the Paleoproterozoic-Archean basement of the Apiaí-São Roque Domain. As this thermal anomaly rapidly progressed to shallower crustal levels, it started to involve the rocks with younger average crustal residence of the Embu Complex, which would thus probably constitute an allochthonous unit thrust over the para-autochthonous Apiaí-São Roque Domain. We note that the tectonic model summarized by Campanha et al. (2023) admits that the Embu Terrane was accreted to a stable area now sitting at the Brazilian platform to the west in the Tonian (~0.85–0.75 Ma) event. In such configuration, there would be no way to generate the Agudos Grandes Batholith by east-directed subduction; accordingly, Campanha et al. (2023) assume a west-directed subduction to generate the HKCA granite magmatism in the Embu, São Roque and Apiaí domains at 670-600 Ma. This is contrary to most tectonic models for the Neoproteozoic evolution of magmatic arcs in the Mantiqueira Province (e.g., Heilbron et al., 2020). To reconcile with those east-directed subduction models, while still keeping the idea that any ocean between the Embu Terrane and a stable area to the west was consumed before the Ediacaran magmatism, a post-collisional origin would be implied for the Agudos Grandes magmatism.

10. Conclusions

The Agudos Grandes Batholith was built along at least 55 Myr (620-565 Ma) by a succession of intrusions that span four main stages: 1- "syn-orogenic" (620-610 Ma), when the main volume of magmas was intruded, mostly as elongated plutons of metaluminous, high-K calc-alkaline character (Ibiúna, Tapiraí and Rio Taquaral types), and also as Th, REE-rich biotite granites (Itapevi-type) and a single body of two-mica leucogranite (Turvo); 2- "late-orogenic" (605-600 Ma), where circumscribed, zoned, sub-rounded plutons of metaluminous to peraluminous character were intruded, mostly to the north of the batholith axis (the Piedade, Serra dos Lopes and Pilar do Sul plutons); 3- "post-orogenic 1" (~585 Ma), the São Miguel Arcanjo A-type granite, and 4- "post-orogenic 2" (~565 Ma), the Serra da Bateia and Serra da

Queimada elongated A-type plutons.

The batholith intruded the Embu Domain, a tectonic block where two metasedimentary sequences of contrasted deposition age and provenance occur in tectonic contact: the Embu Complex (deposited at ~0.97–0.85 Ma) and the lower-metamorphic grade Votuverava Group (deposited at ~1.4–1.3 Ga); both were affected by a strong ~0.85–0.75 Ga metamorphic event which was probably a reflection of their juxtaposition.

The predominant HKCA granites are relatively mafic-rich porphyritic quartz monzonites and monzogranites which show strongly negative εNd(t) and low $^{206}Pb/^{204}Pb$, requiring the participation of crust with long crustal residence, which is reinforced by the presence of >2.0 Ga inherited zircon. These characteristics suggest that this reservoir is the old (Paleoproterozoic to Archean) basement of the Votuverava Group (and in a regional scale of the Apiaí and São Roque Domains). The mafic-rich character is inconsistent with a pure crustal melt, and requires a component from either mixing with basic mantle-derived magmas (for which no clear evidence is apparent at the level of emplacement) or a cumulate and/or (s.l.) "restite" component (which might respond for the persistence of >85% granite liquid to temperatures as low as 850 °C in Rhyolite-MELTS simulations). High Sr/Y ratios are suggestive of melting in hot zones at the deepest portions of a thickened (up to 65 km) continental crust.

The rapid transition to late-orogenic granites is apparently related to upward movement of the thermal anomaly, which sampled a segment of the middle crust with shorter crustal residence, as indicated by the Nd and Pb isotope signatures; this reservoir might correspond to the Embu Complex (upper plate), implying that the later corresponds to an allochthonous terrane overlying the Votuverava Group and its basement at least in the northern portion of the Embu Domain.

The large volumes of calc-alkaline magma involved in the generation of the Agudos Grandes and other regional batholiths of similar age and composition have led some authors to admit that they are products of ocean subduction and building of a continental magmatic arc (e.g., Campanha et al., 2023; Gonçalves et al., 2016). In the tectonic scenario proposed in recent models, where the Embu Terrane was accreted to a stable are to the west in a ~0.85–0.75 Ga collision (Campanha et al., 2023), this could only result from a west-directed subduction; alternatively, it would imply a post-collisional origin for the entire Agudos Grandes batholith.

The post-orogenic A-type granite magmatism emplaced after a ~15 Myr gap is probably the result of delamination of the thickened lithosphere and ensuing collapse of the orogen (Janasi et al., 2001). The participation of mantle-derived melts can respond for the least negative Nd isotope signatures and younger Pb model ages of these granites, but a component from the lower continental crust is suggested by the large volume of fractionated granites.

CRediT authorship contribution statement

Valdecir de Assis Janasi: Writing – review & editing, Writing – original draft, Methodology, Investigation, Funding acquisition, Conceptualization. **Lucelene Martins:** Writing – review & editing, Methodology, Investigation, Conceptualization. **Adriana Alves:** Writing – review & editing, Methodology, Investigation. **Antonio Simonetti:** Writing – review & editing, Methodology. **Renato Henrique-Pinto:** Writing – review & editing, Investigation.

Declaration of competing interest

The authors declare that they have no known competing financial interests or personal relationships that could have appeared to influence the work reported in this paper.

Data availability

Data will be made available on request.

Acknowledgements

Our work in the granite magmatism of SE Brazil has been financed by successive grants from Fapesp (15/01817-6 and 19/17550-0). Map of the Agudos Grandes Batholith was a product of fieldwork cooperation by several colleagues, among which Renato J. Leite, Antonio Carlos Vasconcellos and Silvio Vlach. We thank Larry M. Heaman for support on U–Pb dating at UA-Edmonton, Canada. VAJ acknowledges a CNPq Research Productivity scholarship 306102/2019-6. We thank two anonymous reviewers for insightful suggestions that helped improve our manuscript.

Appendix A. Supplementary data

Supplementary data to this article can be found online at https://doi.org/10.1016/j.jsames.2023.104570.

References

Alves, A., Janasi, V.A., Campos Neto, M.C., 2016. Sources of granite magmatism in the Embu Terrane (Ribeira Belt, Brazil): Neoproterozoic crust recycling constrained by elemental and isotope (Sr-Nd-Pb) geochemistry. J. S. Am. Earth Sci. 68, 205–223. https://doi.org/10.1016/j.jsames.2015.10.014.

Barnes, C.G., Werts, K., Memeti, V., Ardill, K., 2020. Most granitoid rocks are cumulates: deductions from hornblende compositions and zircon saturation. J. Petrol. 60 (11), 2227–2240. <10.1093/petrology/egaa008>.

Blundy, J., 2022. Chemical differentiation by mineralogical buffering in crustal hot zones. J. Petrol. 63 (7) https://doi.org/10.1093/petrology/egac054.

Brackman, A.J., Schwartz, J.J., 2022. The formation of high-Sr/Y plutons in cordilleran-arc crust by crystal accumulation and melt loss. Geosphere. https://doi.org/10.1130/ges02400.1.

Cabrita, D.I.G., Faleiros, F.M., Cawood, P.A., Campanha, G.A.C., Yogi, M.T.A.G., Wainwright, A.N., Raveggi, M., Almeida, V.V., 2021. Petrochronological constraints and tectonic implications of Tonian metamorphism in the Embu complex, Ribeira belt, Brazil. Precambrian Res. 363, 106315 https://doi.org/10.1016/j.precamres.2021.106315.

Campanha, G.A.C., Brito Neves, B.B., 2004. Frontal and oblique tectonics in the Brazilian Shield. Episodes 27 (4), 255–259.

Campanha, G.A.C., Faleiros, F.M., Cawood, P.A., Cabrita, D.I.G., Ribeiro, B.V., Basei, M.A.S., 2019. The Tonian Embu complex in the Ribeira belt (Brazil): revision, depositional age and setting in Rodinia and west Gondwana. Precambrian Res. 320, 31–45. https://doi.org/10.1016/j.precamres.2018.10.010.

Campanha, G.A.C., Faleiros, F.M., Cabrita, D.I.G., Ribeiro, B.V., Cawood, P.A., 2023. The southern Ribeira Belt in Western Gondwana: a record of a long-lived continental margin and terrane collage. J. S. Am. Earth Sci. 127, 104404 https://doi.org/10.1016/j.jsames.2023.104404.

Carvalho, B.B., Sawyer, E.W., Janasi, V.A., 2017. Enhancing maficity of granitic magma during anatexis: entrainment of infertile mafic lithologies. J. Petrol. 58 (7), 1333–1362. <10.1093/petrology/egx056>.

Castro, A., 2014. The off-crust origin of granite batholiths. Geosci. Front. 5 (1), 63–75.

Chapman, J.B., Ducea, M.N., DeCelles, P.G., Profeta, L., 2015. Tracking changes in crustal thickness during orogenic evolution with Sr/Y: an example from the North American Cordillera. Geology 43 (10), 919–922. https://doi.org/10.1130/g36996.1.

Chappell, B.W., White, A.J.R., Wyborn, D., 1987. The importance of residual source material (restite) in granite petrogenesis. J. Petrol. 28 (6), 1111–1138. https://doi.org/10.1093/petrology/28.6.1111.

Clemens, J.D., Stevens, G., Farina, F., 2011. The enigmatic sources of I-type granites: the peritectic connexion. Lithos 126 (3–4), 174–181.

Collins, W.J., Huang, H.-Q., Jiang, X., 2016. Water-fluxed crustal melting produces Cordilleran batholiths. Geology 44 (2), 143–146.

Coutinho, J.M.V., 1972. Petrologia do pré-Cambriano em São Paulo e arredores, vol. 3. Boletim do Instituto de Geociências e Astronomia, pp. 5–99.

Ferreira, F.J.F., Janasi, V.A., Vlach, S.R.F., 1991. Comportamento aerogamaespectrométrico e aeromagnetométrico dos principais granitoides de parte dos Domínios Embu e São Roque, SP. In: II Simpósio de Geologia do Sudeste. Brazilian Geological Society, São Paulo, SP, Brazil, Atas, pp. 149–150.

Frost, B.R., Barnes, C.G., Collins, W.J., Arculus, R.J., Ellis, D.J., Frost, C.D., 2001. A geochemical classification for granitic rocks. J. Petrol. 42 (11), 2033–2048.

Gonçalves, L., Alkmim, F.F., Pedrosa-Soares, A.C., Dussin, I.A., Valeriano, C.d.M., Lana, C., Tedeschi, M., 2016. Granites of the intracontinental termination of a magmatic arc: an example from the Ediacaran Araçuaí orogen, southeastern Brazil. Gondwana Res. 36, 439–458. https://doi.org/10.1016/j.gr.2015.07.015.

Gromet, P., Silver, L.T., 1987. REE variations across the peninsular ranges batholith: implications for batholithic petrogenesis and crustal growth in magmatic arcs. J. Petrol. 28 (1), 75–125.

Halla, J., 2018. Pb isotopes–a multi-function tool for assessing tectonothermal events and crust-mantle recycling at late Archaean convergent margins. Lithos 320, 207–221.
Harrison, T.M., Watson, E.B., 1984. The behavior of apatite during crustal anatexis: equilibrium and kinetic considerations. Geochem. Cosmochim. Acta 48 (7), 1467–1477.
Hasui, Y., Sadowski, G.R., 1976. Evolução Geológica do Pré-cambriano na região sudeste do estado de São Paulo. São Paulo. Rev. Bras. Geociencias 6, 182–200.
Heilbron, M., Pedrosa-Soares, A.C., Campos Neto, M.C., Silva, L.C., Trouw, R.A.J., Janasi, V.A., 2004. A província Mantiqueira. In: Mantesso-Neto, V., Bartorelli, A., Brito Neves, B.B. (Eds.), Geologia do Continente Sul-americano: Evolução da Obra de Fernando Flávio Marques de Almeida, pp. 203–234. Beca.
Heilbron, M., de Morisson Valeriano, C., Peixoto, C., Tupinambá, M., Neubauer, F., Dussin, I., Corrales, F., Bruno, H., Lobato, M., Horta de Almeida, J.C., Guilherme do Eirado Silva, L., 2020. Neoproterozoic magmatic arc systems of the central Ribeira belt, SE-Brazil, in the context of the West-Gondwana pre-collisional history: a review. J. S. Am. Earth Sci. 103, 102710 https://doi.org/10.1016/j.jsames.2020.102710.
Henrique-Pinto, R., Janasi, V.A., Vasconcellos, A.C.B.C., Sawyer, E.W., Barnes, S.J., Basei, M.A.S., Tassinari, C.C.G., 2015. Zircon provenance in meta-sandstones of the São Roque domain: implications for the proterozoic evolution of the Ribeira belt, SE Brazil. Precambrian Res. 256, 271–288. https://doi.org/10.1016/j.precamres.2014.11.014.
Hildebrand, R.S., Whalen, J.B., 2017. The Tectonic Setting and Origin of Cretaceous Batholiths within the North American Cordillera: the Case for Slab Failure Magmatism and its Significance for Crustal Growth. Geological Society of America Special Publication, p. 532.
Hu, F., Ducea, M.N., Liu, S., Chapman, J.B., 2017. Quantifying crustal thickness in continental collisional belts: global perspective and a geologic application. Sci. Rep. 7 (1), 7058. https://doi.org/10.1038/s41598-017-07849-7.
Jacob, J.-B., Moyen, J.-F., Fiannacca, P., Laurent, O., Bachmann, O., Janoušek, V., Farina, F., Villaros, A., 2021. Crustal melting vs. fractionation of basaltic magmas: Part 2, Attempting to quantify mantle and crustal contributions in granitoids. Lithos, 106292. https://doi.org/10.1016/j.lithos.2021.106292.
Janasi, V.A., Leite, R.J., van Schmus, W.R., 2001. U-Pb chronostratigraphy of the granitic magmatism in the Agudos Grandes batholith (west of Sao Paulo, Brazil) – implications for the evolution of the Ribeira belt. J. S. Am. Earth Sci. 14 (4), 363–376.
Leite, R.J., Janasi, V.A., Martins, L., 2006. Contamination in mafic mineral-rich calc-alkaline granites: a geochemical and Sr-Nd isotope study of the Neoproterozoic Piedade Granite, SE Brazil. An. Acad. Bras. Cienc. 78 (2), 345–371.
Leite, R.J., Heaman, L.M., Janasi, V.A., Martins, L., Creaser, R.A., 2007a. The late- to postorogenic transition in the Neoproterozoic Agudos Grandes granite batholith (apiai domain, SE Brazil): constraints from geology, mineralogy, and U-Pb geochronology. J. S. Am. Earth Sci. 23 (2–3), 193–212.
Leite, R.J., Janasi, V.A., Creaser, R.A., Heaman, L.M., 2007b. The late- to postorogenic transition in the Apiaí domain, SE Brazil: constraints from the petrogenesis of the Neoproterozoic Agudos Grandes granite batholith. J. S. Am. Earth Sci. 23 (2–3), 213–235.
Maniar, P.D., Piccoli, P.M., 1989. Tectonic discrimination of granitoids. Geol. Soc. Am. Bull. 101 (5), 635–643.
Maurer, V.C., Alves, A., Campos Neto, M.C., 2015. Characterization of the Rio Capivari complex, basement of the Embu terrane: geochemical and geochronological constraints. In: 8th Hutton Symposium on Granites and Related Rocks, Florianópolis, Brazil, Abstracts Volume.
Mcdonough, W.F., Sun, S.-S., 1995. The composition of the Earth. Chem. Geol. 120, 228.
Meira, V.T., García-Casco, A., Juliani, C., Almeida, R.P., Schorscher, J.H.D., 2015. The role of intracontinental deformation in supercontinent assembly: insights from the Ribeira Belt, Southeastern Brazil (Neoproterozoic West Gondwana). Terra. Nova 27 (3), 206–217. https://doi.org/10.1111/ter.12149.
Moyen, J.-F., Janoušek, V., Laurent, O., Bachmann, O., Jacob, J.-B., Farina, F., Fiannacca, P., Villaros, A., 2021. Crustal melting vs. fractionation of basaltic magmas: Part 1, the bipolar disorder of granite petrogenetic models. Lithos, 106291. https://doi.org/10.1016/j.lithos.2021.106291.
Passarelli, C.R., Verma, S.K., McReath, I., Basei, M.A.S., Siga, O., 2019. Tracing the history from Rodinia break-up to the Gondwana amalgamation in the Embu terrane, southern Ribeira belt, Brazil. Lithos 342–343, 1–17. https://doi.org/10.1016/j.lithos.2019.05.024.
Prazeres Filho, H.J., Harara, O.M., Basei, M.A.S., Passarelli, C.R., Siga Jr., O., 2003. Litoquímica, geocronologia U-Pb e geologia isotópica (Sr-Nd-Pb) das rochas graníticas dos batólitos Cunhaporanga e Três Córregos na porção sul do Cinturão Ribeira, Estado do Paraná. Geol. Usp. Série Científica 3, 51–70.
Siégel, C., Bryan, S.E., Allen, C.M., Gust, D.A., 2018. Use and abuse of zircon-based thermometers: a critical review and a recommended approach to identify antecrystic zircons. Earth Sci. Rev. 176, 87–116. https://doi.org/10.1016/j.earscirev.2017.08.011.
Stacey, J.S., Kramers, J.D., 1975. Approximation of terrestrial lead isotope evolution by a two-stage model. Earth Planet Sci. Lett. 26 (2), 207–221.
Vermeesch, P., 2018. IsoplotR: a free and open toolbox for geochronology. Geosci. Front. 9, 1479–1493. https://doi.org/10.1016/j.gsf.2018.04.001.
Watson, E.B., Harrison, T.M., 1983. Zircon saturation revisited: temperature and composition effects in a variety of crustal magma types. Earth Planet Sci. Lett. 64 (2), 295–304.
Whalen, J.B., Hildebrand, R.S., 2019. Trace element discrimination of arc, slab failure, and A-type granitic rocks. Lithos 348–349, 105179. https://doi.org/10.1016/j.lithos.2019.105179.
Zartman, R.E., Doe, B.R., 1981. Plumbotectonics—the model. Tectonophysics 75 (1), 135–162. https://doi.org/10.1016/0040-1951(81)90213-4.